Interim Report No.1

Experiments with mutually coupled arrays of Josephson junctions*

A.A. Abdumalikov, P. Caputo† and A. V. Ustinov

Physikalisches Institut III, Universität Erlangen-Nürnberg
D-91054 Erlangen, Germany

* Supported by European Office of Aerospace Research and Development (EOARD)
under Contract F61775-00-WE004
† Current address: Universita' degli Studi di Salerno Dipartimento di Fisica Via. S. Allende,
I-84081 Baronissi (Salerno) Italy

September 2000

REPORT DOCUMENTATION PAGE

Form Approved OMB No. 0704-0188

1. REPORT DATE (DD-MM-YYYY)	2. REPORT TYPE	3. DATES COVERED (FROM - TO)
28-09-2001	Final	29-08-2000 to 29-08-2001

4. TITLE AND SUBTITLE
Experiments with Mutually Coupled Arrays of Josephson Junctions
Unclassified

5a. CONTRACT NUMBER
F61775-00-WEO04

5b. GRANT NUMBER

5c. PROGRAM ELEMENT NUMBER

6. AUTHOR(S)
Ustinov, Alexey ;

5d. PROJECT NUMBER

5e. TASK NUMBER

5f. WORK UNIT NUMBER

7. PERFORMING ORGANIZATION NAME AND ADDRESS
University of Erlangen-Nuremberg
Erwin-Rommel-Str.1
Erlangen, Germany91058

8. PERFORMING ORGANIZATION REPORT NUMBER

9. SPONSORING/MONITORING AGENCY NAME AND ADDRESS
EOARD
PSC 802 BOX 14
FPO, 09499-0014

10. SPONSOR/MONITOR'S ACRONYM(S)

11. SPONSOR/MONITOR'S REPORT NUMBER(S)

12. DISTRIBUTION/AVAILABILITY STATEMENT
APUBLIC RELEASE
,

13. SUPPLEMENTARY NOTES

14. ABSTRACT

This report results from a contract tasking University of Erlangen-Nuremberg as follows: The contractor will investigate triangular arrays of Josephson tunnel junctions which have proven suitable for high frequency applications in the mm and sub-mm range. Yukon (AFRL) and Lin have designed an active antenna array based on 2D triangular arrays as oscillators. Synchronization between the oscillators (or sub-arrays) is provided by a phase shifter consisting of a parallel Josephson junction chain. The contractor has proposed an experiment based on a circuit made of two sub-arrays coupled by the phase shifter. Radiation from two subarrays will be coupled into a fin-line antenna and the emitted power will be studied as a function of a phase shift provided by the Josephson junction chain placed between the sub-arrays. Alternative methods using on-chip radiation detectors will be also explored.

15. SUBJECT TERMS
EOARD; Josephson junctions; Millimeterwave technology; Microwave source

16. SECURITY CLASSIFICATION OF:			17. LIMITATION OF ABSTRACT	18. NUMBER OF PAGES	19. NAME OF RESPONSIBLE PERSON
a. REPORT	b. ABSTRACT	c. THIS PAGE	Public Release	28	Fenster, Lynn lfenster@dtic.mil
Unclassified	Unclassified	Unclassified			19b. TELEPHONE NUMBER International Area Code Area Code Telephone Number 703767-9007 DSN 427-9007

REPORT DOCUMENTATION PAGE

Form Approved OMB No. 0704-0188

1. REPORT DATE *(DD-MM-YYYY)*	2. REPORT TYPE	3. DATES COVERED *(From – To)*
28-09-2001	Final Report	29 August 2000 - 29-Aug-01

4. TITLE AND SUBTITLE

Experiments with mutually coupled arrays of Josephson junctions

5a. CONTRACT NUMBER
F61775-00-WE004

5b. GRANT NUMBER

5c. PROGRAM ELEMENT NUMBER

6. AUTHOR(S)

Prof. Dr. Alexey Ustinov

5d. PROJECT NUMBER

5d. TASK NUMBER

5e. WORK UNIT NUMBER

7. PERFORMING ORGANIZATION NAME(S) AND ADDRESS(ES)
University of Erlangen-Nuremberg
Erwin-Rommel-Str. 1
Erlangen 91058
Germany

8. PERFORMING ORGANIZATION REPORT NUMBER
N/A

9. SPONSORING/MONITORING AGENCY NAME(S) AND ADDRESS(ES)

EOARD
PSC 802 BOX 14
FPO 09499-0014

10. SPONSOR/MONITOR'S ACRONYM(S)

11. SPONSOR/MONITOR'S REPORT NUMBER(S)
SPC 00-4004

12. DISTRIBUTION/AVAILABILITY STATEMENT

Approved for public release; distribution is unlimited.

13. SUPPLEMENTARY NOTES

14. ABSTRACT

This report results from a contract tasking University of Erlangen-Nuremberg as follows: The contractor will investigate triangular arrays of Josephson tunnel junctions which have proven suitable for high frequency applications in the mm and sub-mm range. Yukon (AFRL) and Lin have designed an active antenna array based on 2D triangular arrays as oscillators. Synchronization between the oscillators (or sub-arrays) is provided by a phase shifter consisting of a parallel Josephson junction chain. The contractor has proposed an experiment based on a circuit made of two sub-arrays coupled by the phase shifter. Radiation from two sub-arrays will be coupled into a fin-line antenna and the emitted power will be studied as a function of a phase shift provided by the Josephson junction chain placed between the sub-arrays. Alternative methods using on-chip radiation detectors will be also explored.

15. SUBJECT TERMS
EOARD, Josephson junctions, Millimeterwave technology, Microwave source

16. SECURITY CLASSIFICATION OF:			17. LIMITATION OF ABSTRACT	18, NUMBER OF PAGES	19a. NAME OF RESPONSIBLE PERSON
a. REPORT	b. ABSTRACT	c. THIS PAGE			Christopher Reuter, Ph. D.
UNCLAS	UNCLAS	UNCLAS	UL	27	19b. TELEPHONE NUMBER *(Include area code)* +44 (0)20 7514 4474

Contents

Abstract

High frequency properties of triangular arrays of Josephson tunnel junctions operating in a magnetic field are studied experimentally. Previously reported experiments have shown that the horizontal junctions of a triangular array can deliver a considerable output power in the frequency range 90-120 GHz that has been detected by a room temperature receiver. Within the current project, we have designed a new circuitry to characterize the emitted radiation from triangular arrays by means of an on-chip detection. The fabricated circuits are intended to cover the band from 60 to 200 GHz. First measurements of these circuits are presented in this report.

Chapter 1

Introduction

Josephson junctions are naturally voltage-to-frequency transducers. When a dc voltage (V) is established across the superconducting electrodes, the junction radiates electromagnetic waves at a frequency (ν) determined by the Josephson relation:

$$\nu = \frac{2e}{h}V,$$

where e is the electron charge and h is the Plank constant. In general the typical power levels of the emitted radiation are very small. In order to use this power in practical applications one should collect coherent radiation from many junctions. If the junctions are independent, it is difficult to tune radiation frequencies to be same for every one. To avoid this problem one should use a system where each junction interacts with the others, allowing the junctions to synchronize at one frequency. One of these systems is represented by arrays of Josephson junctions, and particularly by triangular arrays. Triangular arrays of Josephson junctions operating in an applied magnetic field have been proposed for obtaining useful radiation power in mm and sub-mm ranges [1, 2, 3]. At the applied field corresponding to half a flux quantum in every cell ($f = 0.5$), the junctions transverse to the forcing current oscillate about their equilibrium state rather than rotating over 2π, yielding an rf power with very small content of higher harmonics. Numerical simulations have shown that the entire array operating near the resonant frequency $\omega_{LC/3}$ can be phase locked, allowing maximum rf power to be generated. Previous experiments with triangular rows [4, 5, 6] have already demonstrated radiation from the *horizontal* junctions, although they are not subjected to the driving force from the external bias current. The radiation frequency is equal to the Josephson frequency of the *vertical* junctions.

Challenging issue is the detection of radiation at high frequencies. In our previous experiments we have successfully used a room temperature receiver based on the superetherodyne technique, in which the signal from the horizontal Josephson junctions was picked up by a fin-line antenna and transmitted via a waveguide to the receiver. Within the present contract we intend to develop and experimentally demonstrate another detection technique using on-chip radiation detection scheme. The IREE group has recently extensively used and developed the on-chip detection for operation in the superconducting integrated receivers [7]. Essentially, the on-chip detector consists of a small SIS type junction connected to a radiation source via a transmission line with a dc-break. The design of our circuit was prepared on the basis of the calculations made by Sergey Shitov using our junction parameters [8].

In this report, we describe the on-chip detection circuit design and present first results of experiments performed on single-row triangular arrays with an on-chip detector.

Chapter 2

Experiments

2.1 Junction and array layout

The samples according to our micro-design and specification were prepared at the foundry of the Institute for Physical High Technology (IPHT) in Jena, Germany. The parameters of the junctions of the array and detector are the same. The size of each junction is about $9\mu\text{m}^2$. The cell size is about $S = 240\mu\text{m}^2$. The row consists of ten square cells. The horizontal junctions of the row are connected to the detector through a transmission line with a dc-break. As an example of the geometry, in Fig. 1 we show a schematic view of a 6-cell array coupled to an on-chip detector, and also a photograph of the real circuit.

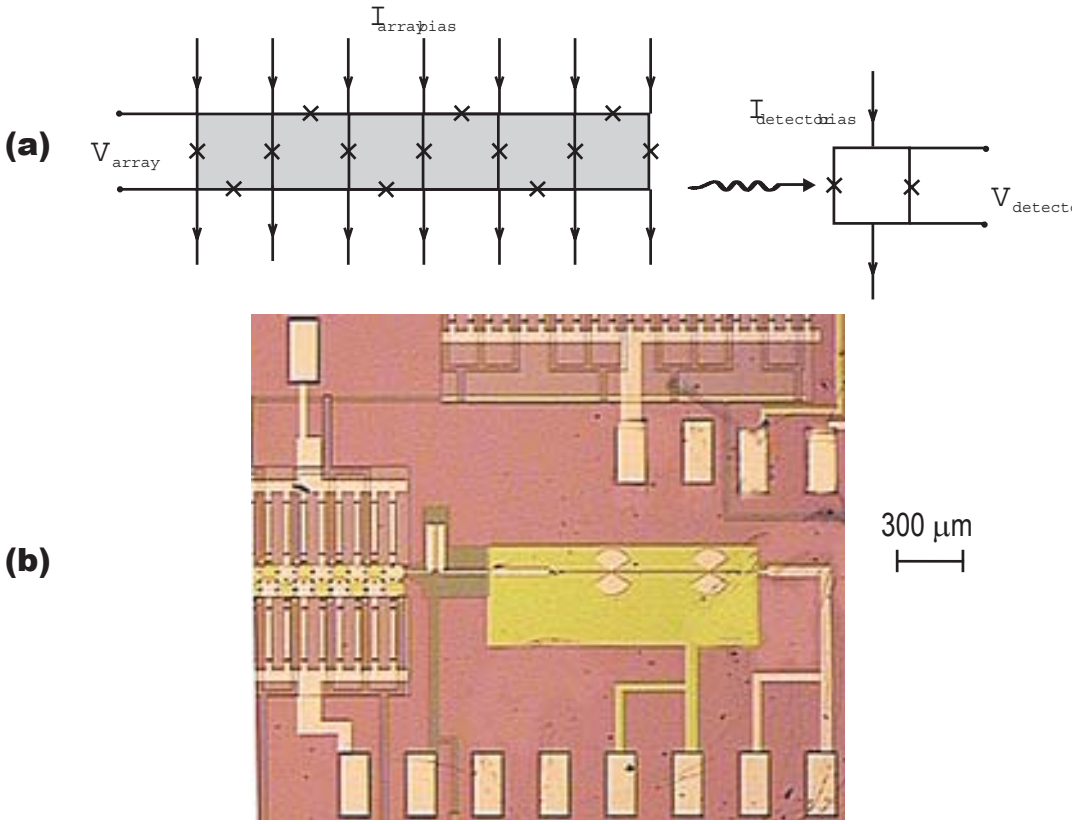

Figure 1: Schematic view (a) and optical image (b) of an array coupled to an on-chip detector.

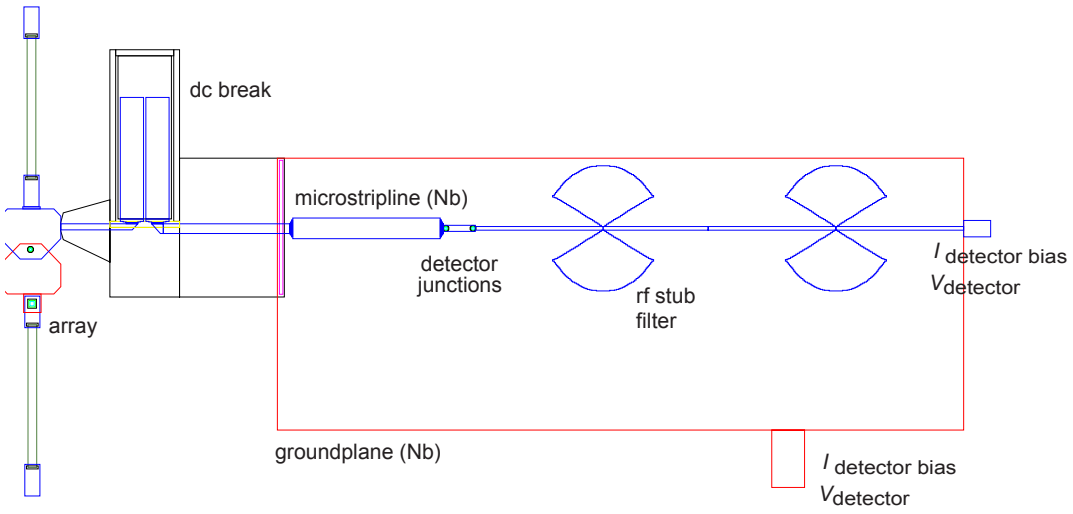

Figure 2: Layout of the coupling circuit and of the detector.

The external bias current ($I_{\mathrm{array\_bias}}$) is uniformly injected at each node of the array via resistors (along the vertical direction of, Fig. 1b), and a voltage response (V_{array}) is measured across the vertical junctions. The detector consists of two parallel connected small Josephson junctions. The detector is independently biased with a current $I_{\mathrm{detector\_bias}}$ and a voltage V_{detector} is measured. The discreteness of the array is expressed in terms of the parameter $\beta_{\mathrm{L}} = 2\pi\frac{LI_{\mathrm{c}}}{\Phi_0}$, where L is the self-inductance of the elementary cell, I_{c} is the critical current of the single junction, Φ_0 is the flux quantum. The cell inductance can be estimated as $L = 1.25\mu_0\sqrt{S}$. The damping of the junctions is defined in terms of the McCumber parameter, $\beta_{\mathrm{C}} = 2\pi\frac{I_{\mathrm{c}}R_{\mathrm{N}}^2C}{\Phi_0}$. Here R_N is sub-gap resistance and C is the junction capacitance.

2.2 On-chip rf coupling circuitry

A layout of the circuit used to couple the radiation emitted from the array to a detector is sketched in Fig. 2. The "horizontal" line of the array is coupled to the on-chip detector through a transmission line. The transmission line between the array and the detector consists of three main parts: microstrip, dc-break, microstrip with varying width [7]. The dc-break is made as a slot line. Behind the detector, there are two radial stub filters which prevent the leak of the radiation power via the detector leads.

This circuit was designed to optimize impedance matching between array and detector, according to the calculations of S. Shitov [8]. In these calculations, the impedance of the array is estimated with shorted end. Then, using well known formulas for impedance transformation between two points (input and output) of microstrips (or slot lines), one can calculate the impedance at the output Z_{out} knowing the impedance at the input Z_{in} of the microstrip lines, and vise versa (Fig. 3)

$$Z_{\mathrm{out}} = Z_0\frac{Z_{\mathrm{in}} + Z_0\tanh(\beta x)}{Z_0 + Z_{\mathrm{in}}\tanh(\beta x)}, \tag{1}$$

where Z_0 is the characteristic impedance of the line, β is the imaginary part of the propagation constant of the line. Z_0 and β depend on the width and length of the line, on the frequency of

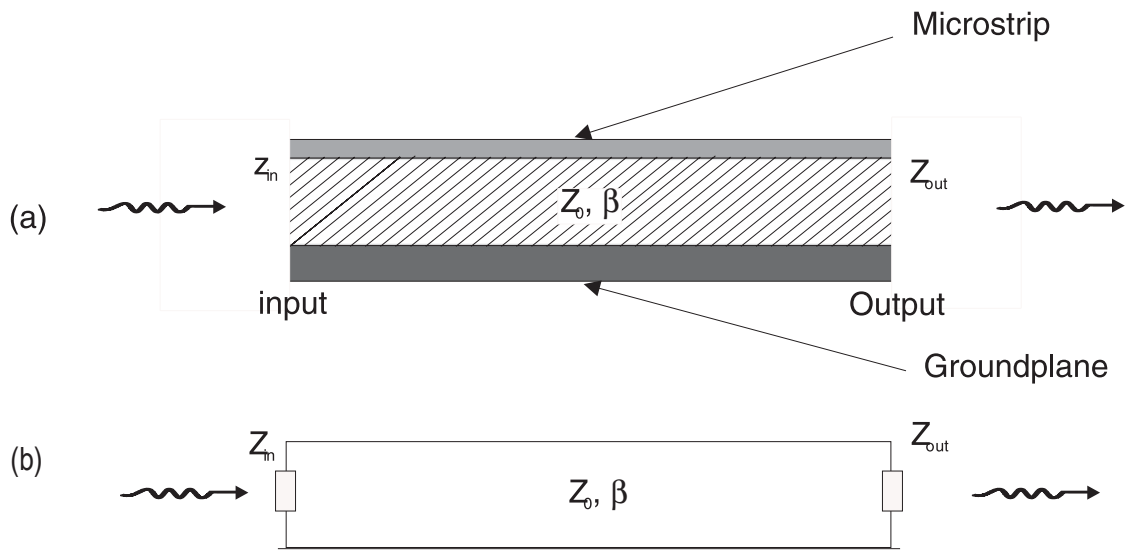

Figure 3: Microstrip line (a) and its schematic view (b).

the electromagnetic wave for which impedances are calculated, and on the dielectric constant of the medium between the electrodes of the line. Eq. (1) includes losses in the line and is obtained in the limit of a quasi-static analysis. In this limit, the width of the line should be much smaller than the electromagnetic wavelength. If the wavelength is comparable with the width of the line, one should take into account fringe (edge) effects. This effect may change the characteristic impedance and the propagation constant. These changes can be taken into account by using an effective width and an effective dielectric constant instead of the width of the line and the dielectric constant of the medium. In the calculation of the impedance transformation through Josephson junction (in our case junction array), one should take into account that the velocity of electromagnetic waves in Josephson junction is equal to the Swihart velocity. The matching coefficient is calculated using standard formulas:

$$C(Z_1, Z_2) = \frac{4Re(Z_1)Re(Z_2)}{|Z_1 + Z_2|^2} 100\%; \tag{2}$$

$$C(Z_1, Z_2) = -20Log\left(\frac{4Re(Z_1)Re(Z_2)}{|Z_1 + Z_2|^2}\right), \tag{3}$$

in per cent and in dB, respectively. In these formulas Z_1 and Z_2 are the transformed impedances to the considered point from two ends of the system. For calculating impedance transformation through the whole array, one should assume each cell as a single impedance and that the impedances of all cells are connected in parallel. Finally, for the studied system we obtained the dependence of the matching coefficient (between the array and the detector) on the frequency that is shown in Fig. 4.

Figure 4(a) is calculated by taking the input (array) impedance as lumped active 10 Ω. From Fig. 4(a) one can see that in this case the impedance matching for the measured system is rather good for a wide band of frequencies (60 - 200 GHz). In Fig. 4(b) we show the full calculation of the real array matching coefficient. It is obtained by transforming the impedances junction by junction, starting from the shorted end of the strip line. The frequency $\nu_0 = 85$ GHz is marked, as there is a local maximum of the matching coefficient. This maximum is very close to the frequency at which actually we observed radiation in

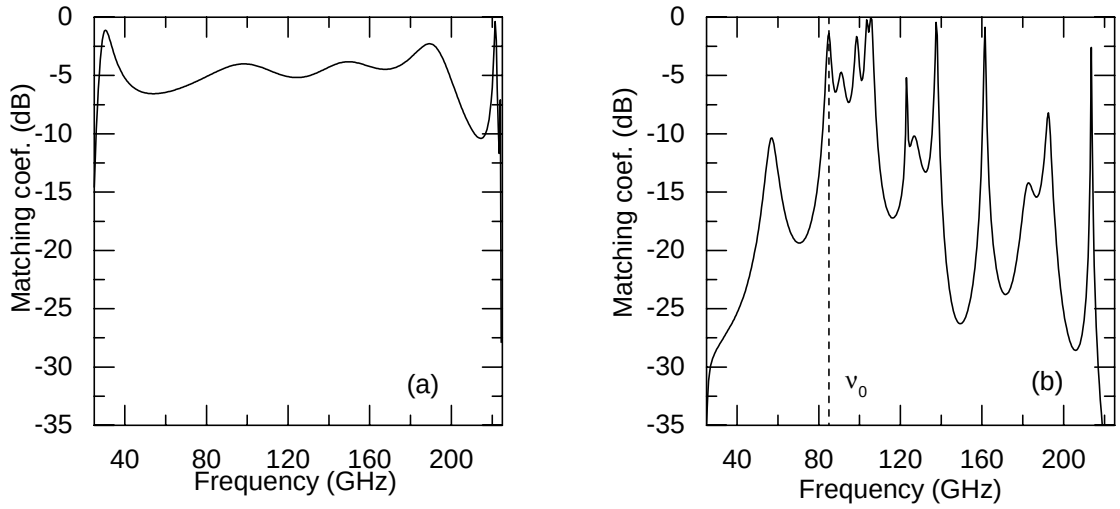

Figure 4: Matching coefficient dependence on frequency: (a) input impedance is assumed to be 10 Ohm; (b) input impedance is taken as the transformed impedance of the array with shorted end.

fabricated circuits. There are also many other peaks in the graph, but these frequencies are away from the frequency of the resonant emission of the array and indeed no radiation was observed.

2.3 Measurements

Measurements were performed in the presence of a magnetic field having components both perpendicular and parallel to the array plane. The parallel field ($H_{\|}$) is applied to decrease the critical current of the Josephson junctions. In this way, without changing temperature, we are able to tune the parameters β_c and β_L to lower values for which the existence of the step in the I-V curve was predicted. The perpendicular field ($H_{\perp}$) is applied as usual to change the frustration through the array cells. In order to decrease external noise, we applied the dc bias through RC-filters with cut-off frequency of about 1 MHz. The filters were mounted on the top of the deep-stick at room temperature. Residual dc magnetic field was screened by a cryoperm shield.

The dc analysis consists of investigation of the current-voltage (I-V) characteristics of the array and the detector at different values of the magnetic field. The array's critical current pattern versus perpendicular magnetic field ($H_{\perp}$) in the presence of a constant parallel magnetic field ($H_{\|}$) is also checked. In Fig. 5(a), it is reported a typical I-V curve of the array, with no magnetic field applied. Fig. 5(b) shows modulation of the array critical current versus the perpendicular field. We notice the typical periodic behavior, although the maximum current is found not at zero field due to the presence of a residual flux. In Fig. 6 we show an I-V curve of the detector. The critical current is suppressed due to trapped flux.

In the presence of frustration, for small region of (β_L, β_C)-plane we observed a step in the I-V curves of the array. This step appears at the voltage of about 120-170 μV. To enhance radiation power, we had to increase temperature or suppress critical current, so that

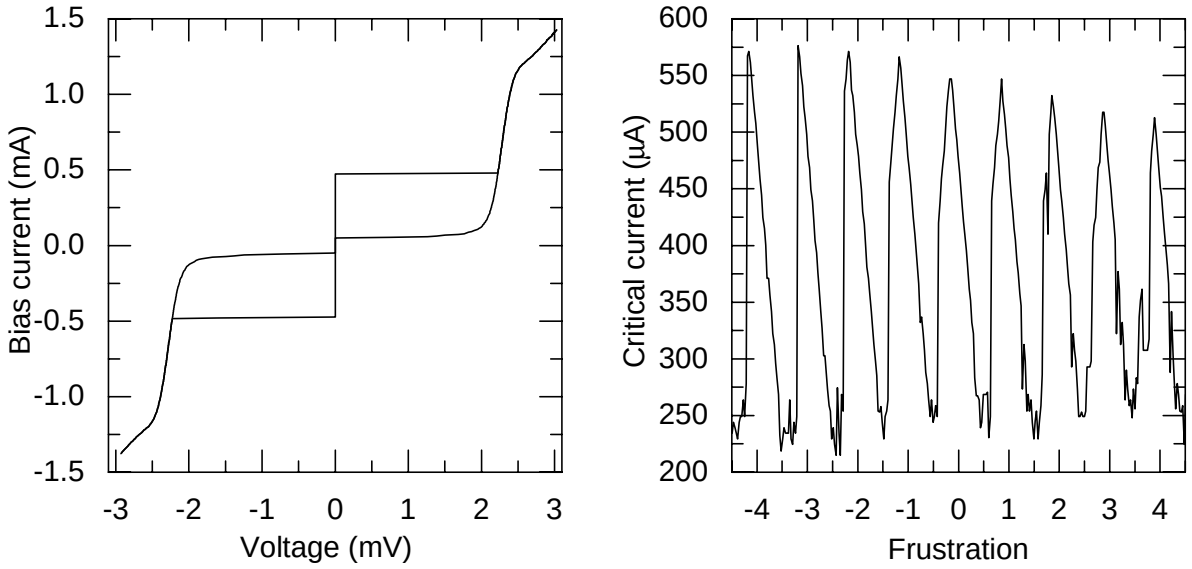

Figure 5: DC characteristics of the array: (a) I-V curve, $H_{||} = 0$ and $H_{\perp} = 0$; (b) $I_c(H_{\perp})$, $H_{||} = 0$.

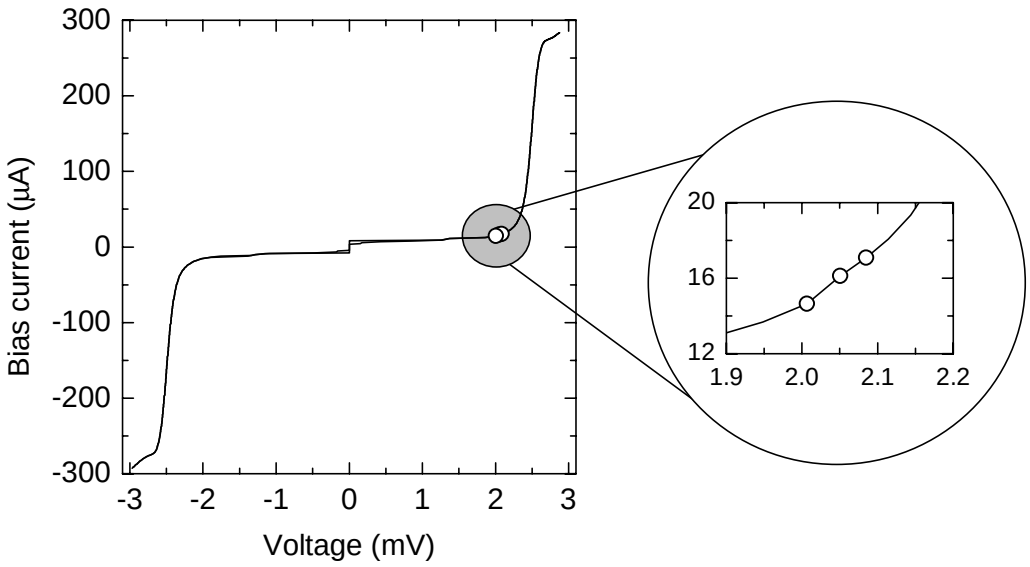

Figure 6: Current-voltage characteristic of the detector, $H_{||} = 0$ $H_{\perp} = 0$. The inset shows the bias points at which the detector was biased during measurements (see text).

parameters β_C and β_L go down to about 500 and 1, respectively.

Under the influence of electromagnetic radiation with frequency ν coming from the array, the I-V curve of the detector is expected to change its form because of two phenomena. First of these phenomena manifests as Shapiro steps at the voltage $V = \frac{mh\nu}{2e}$, where $m = \pm 1, \pm 2....$

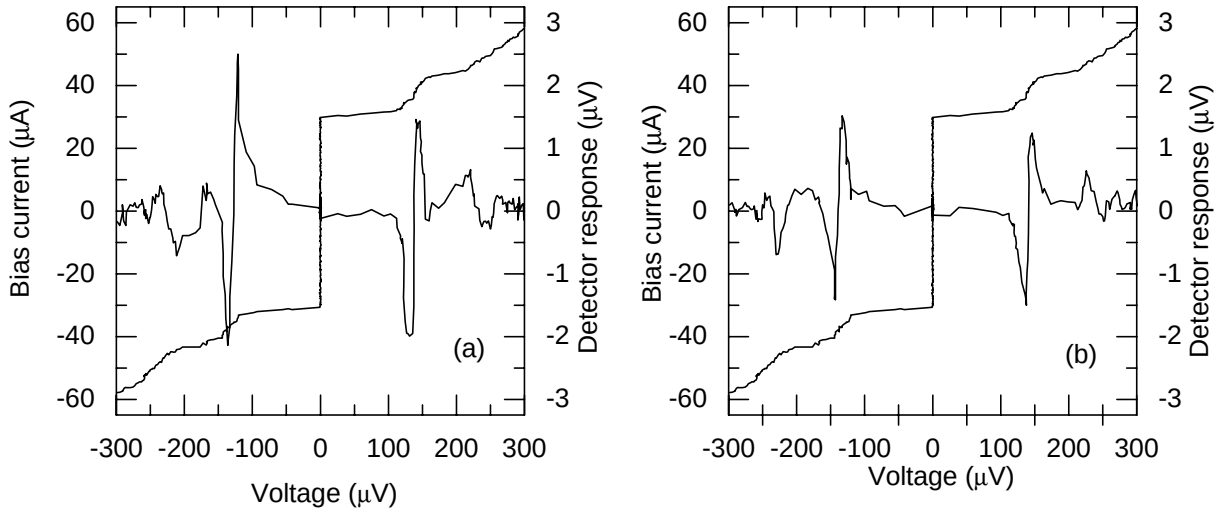

Figure 7: I-V curves and detector responses for: (a) $I_d = 16.11\ \mu A$, $I_{\rm mod} = 3.8\mu A$; (b) $I_d = 17.2\ \mu A$, $I_{\rm mod} = 3.8\mu A$.

Second phenomenon is the so called *photon-assisted tunneling* [9]. Photon-assisted tunneling takes place when the external radiation excites quasiparticles, so that they can tunnel through the tunnel barrier. This process manifests itself on the I-V curve as current steps around the gap voltage. The voltages of the steps are determined by the frequency of the radiation as $V_{PAT} = 2\frac{\Delta}{e} \pm \frac{n\hbar\omega}{e}$, where n is number of photons which are needed to excite each quasiparticle so that it can tunnel. The step height in current is determined by the power of radiation. In our system, we can estimate the radiation power emitted by the array by measuring changes in the I-V curve of the detector. To avoid ground loops, which can induce large noise, we used two current sources with different grounds for biasing the array and the detector.

We noticed that the I-V curve of the detector was changing very little under the effect of the array radiation. Thus, we have chosen a sensitive method of detection of small voltage changes. The response of the detector to the radiation from the array was measured with a lock-in amplifier. We have modulated the array bias current ($I_{\rm array\ bias}$) with a low frequency ($\nu_{\rm mod}$) and small amplitude ($I_{\rm A}$) signal, such that $\nu_{\rm mod}$is about several hundred Herz and $I_{\rm A} \ll I_{\rm array\ bias}$. The output signal measured by the lock-in amplifier is then the averaged response of the detector at the frequency of modulation. While sweeping the array bias current, the detector was biased with a constant current at voltage of about 2 mV, and changes of its voltage due to photon-assisted tunneling were measured. Typical bias point for which we measured radiation are shown in Fig. 6. The results are presented in Fig. 7. In this figure we report the measurements for different two detector currents I. Increasing the modulation amplitude also increases the detector response. However, if the modulation amplitude gets larger than the amplitude of the step in the I-V curve of the array, the response decreases. All our measurements were done at bias points of the detector around the onset of the gap voltage [Fig. 7(a) $V_{\rm detector} = 2.051$ mV, Fig. 7(b) $V_{\rm detector} = 2.085$ mV]. In this region, for smaller currents the response is larger, as expected. The presented measurements

were done for a constant parallel magnetic field $H_{||} = 25.13Oe$, frustration $f = 0.55$ and modulation frequency $\nu_{mod} = 637$ Hz.

From Fig. 7, we estimate the radiation frequency to be in range from about 67 to 73 GHz. We compared these results with matching coefficient calculations and got that the matching is in the range between -4 B and -6 dB for Fig. 4(a) and between -15 dB and -20 dB for Fig. 4(b).

Conclusions

We reported first measurements using an on-chip radiation detection scheme. Radiation emitted by a Josephson tunnel junction arrays consisting of one row of 10 parallel biased cells was detected. Measurements were performed in the presence of magnetic fields applied perpendicular and parallel to the plane of the array. In previous measurements the suppression of the critical current was achieved by increasing the working temperature. That technique allowed to tune the parameters β_L and β_C in a desired range, but was accompanied by large fluctuations of these parameters. In the presented experiments, we suppress the critical current by using a parallel magnetic field which turns to be more convenient and stable. At the perpendicular magnetic field corresponding to half a flux quantum in every cell, the horizontal junctions of the array oscillate about their equilibrium positions. These oscillations radiate a measurable amount of power at the frequency range about 70 GHz, which we successfully detected with the on-chip detector.

Bibliography

[1] S.P. Yukon and N.C.H. Lin, Generation of mode locked pulses using 2D triangular Josephson junction arrays, IEEE Trans. Appl. Supercond., **7**, No.2, pp.3115-3121 (1997)

[2] S.P. Yukon and N.C.H. Lin, Josephson junction phased arrays, IEEE Trans. Appl. Supercond., **9**, No.2, pp.4533-4537 (1999)

[3] S.P. Yukon and N.C.H. Lin, Maximazing microwave power from triangular Josephson junction arrays, IEEE Trans. Appl. Supercond., **9**, No.2, pp.4320-4324 (1999)

[4] P. Caputo, A.V. Ustinov, N.C.H. Lin and S.P. Yukon, Radiation from triangular arrays of Josephson junctions. IEEE Trans. Appl. Supercond., **9**, No.2, pp.4538-4541 (1999)

[5] P. Caputo, A. Duwel, T. P. Orlando, A. V. Ustinov, N. C. H. Lin, S. P. Yukon, Experiment with triangular Arrays of Josephson Junctions, in Proc. of Eur. Conf. on Applied Superconductivity, Eds. H. Koch and S. Knappe, (Publisher: Physikalisch-Technische Bundesanstalt, Braunschweig, 1997), pp. 180-182.

[6] P. Caputo and A. V. Ustinov, Final Report on Analysis of Triangular Arrays of Josephson Tunnel Junctions, contract F61775-98-WE041, May 1999.

[7] V.P. Koshelets and S.V. Shitov, Topical review: Integrated superconducting receivers, Supercond.Sci.Technol. **13** R53-R69. (2000)

[8] S.V. Shitov, unpublished (1998-2000)

[9] N.R. Werthamer, Phys.Rev. **147**, p.255,(1966)

Interim Report No.2

Experiments with mutually coupled arrays of Josephson junctions*

A.A. Abdumalikov, A.V. Veretennikov[1], S.V. Shitov[2] and A. V. Ustinov

Physikalisches Institut III, Universität Erlangen-Nürnberg
D-91054 Erlangen, Germany

[1]Institute of Solid State Physics RAS, 142432, Chernogolovka, Russia

[2]Institute for Radio Engineering and Electronics RAS, Moscow, Russia

* Supported by European Office of Aerospace Research and Development (EOARD)
under Contract F61775-00-WE004

February 2001

Contents

Abstract

New samples were designed for studying resonances of triangular arrays of Josephson junctions in magnetic field. In previously reported experiments it has been shown that horizontal junctions of a triangular array can radiate a considerable output power in a wide range of the frequency which mainly depends on McCumber (β_C) and discreteness (β_L) parameters [1]. This radiation was detected in most cases by a room temperature receiver. In this report we describe our new improved design of on-chip radiation detection circuits that currently are submitted for fabrication at the Institute for Physical High Technology (IPHT) Jena foundry. The second part of this report describes first measurements and new design of samples for radiation detection experiments using the 400-500 GHz superconducting low temperature receiver.

1 Improved on-chip coupling circuits for triangular arrays

In this part we describe our new design of the on-chip detection circuit for studying high frequency properties of triangular arrays of small Josephson junctions. For introduction into the problem we refer to the our previous Interim Report No.1 [2], where the design of on-chip rf coupling circuits and their measurements have first been reported.

Within current project we have designed 3 new circuits for radiation detection by on-chip detectors. Design layout of one of these circuits is presented in Fig 1. All of the circuits consist of five parts: i) radiation source, ii) dc-break, iii) impedance transformer, iv) detector and v) dc-filter based on radial stub.

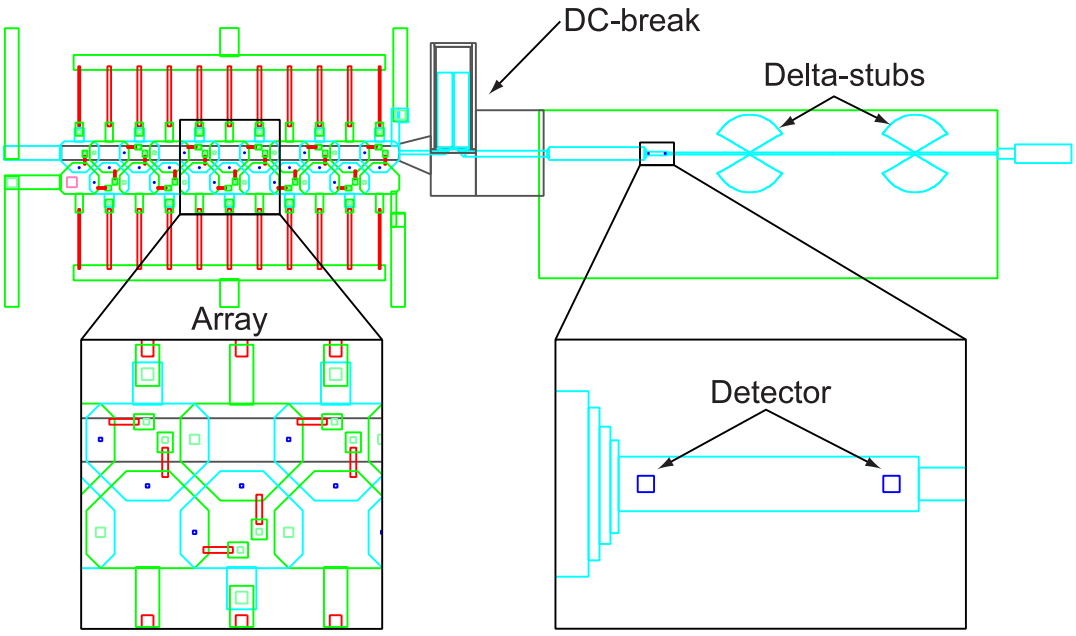

Figure 1: Layout of the array, coupling circuit and detector.

In all 3 cases as a radiation source we used triangular array of Josephson junctions. The array of the first circuit consists of ten cell with three shunted junctions. The shunt resistance is 5 Ohm. The second circuit also consists of ten cell, but the junctions are not shunted. The third circuit is similar to the second one, but its array has only five cells. The dc-break and

array are connected via short transmission line, length and width of which we changed for appropriate impedance matching of the circuit. Parameters of the impedance transformer between dc-break and detector determine the frequency range where radiation detection is possible. The detector contains two small SIS junctions. The radial stub based filters are filtering external noise.

The radiation frequency of our previously prepared samples lyes in the range 60-80 GHz. The critical current density of these samples at 4.2 K was about 300 Amp/cm^2, while for new ordered samples it is expected to be about 100 ± 50 Amp/cm^2. The critical current density determines parameters such as capacitance and resistance of the junctions. The capacitance of the junction determines radiation frequency. In designed samples the radiation frequency is expected to be higher than 80 GHz. We estimated it to be in range $90 - 110$ GHz.

Relative to our first design, we shifted the frequency range of the coupling circuit to higher frequencies around $80 - 120$ GHz. We changed the parameters of the impedance transformer, i.e. widths and lengths of the transmission line segments of which it consists. In Fig. 2(a) we present the calculated matching coefficient for the previous made and currently designed samples. In calculations, of which as a radiation source we took either lumped element of 5 Ohms or an array of shunted junctions. One can see that in the region of interest, the matching coefficient was improved while for higher frequencies it got worse.

The red line in Fig 2(a) corresponds to the array of shunted Josephson junctions. In the frequency range around $\nu_0 = 100$ GHz this curve shows the coupling of about -5 dB. In Fig 2(b) we present the matching coefficient for the other two samples with arrays junctions of which are not shunted. One can see that matching at the preferred frequency ν_0 is worse than it is for first sample, and it is also very nonuniform.

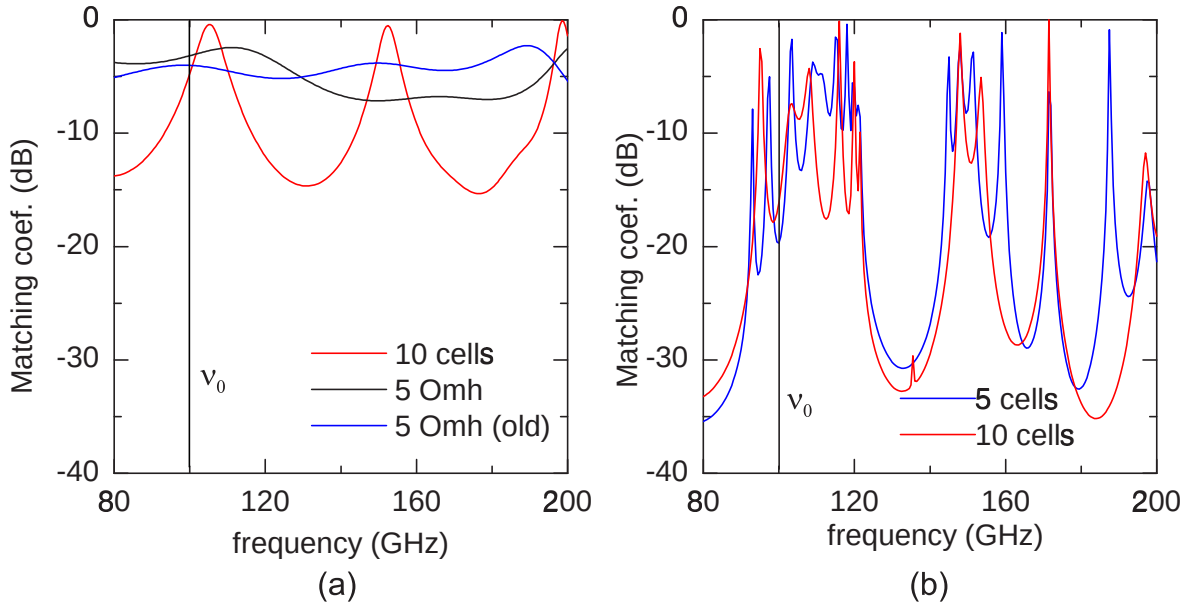

Figure 2: Matching coefficient dependence on frequency: (a) for an array of shunted Josephson junctions and for a lumped element of 5 Ohm; (b) for arrays with 5 and 10 cells having the shorted end.

We did our best to get more flat matching for these samples. Yet it remains very peaked because of much difference between transformed impedances of the arrays and other parts of the samples. But taking into account, that the shunt resistor inductance shifts the resonance

position to lower frequency, for these arrays we expect that resonance step will be in the range $105 - 120$ GHz where we have better matching.

Our previous calculations of the matching ranges have been done for the lumped impedance sources. Now we have also included into calculation matching of the distributed array as it is, taking into account the number of its cells, shorted end, etc. Therefore, we suppose that the characteristics of real arrays will be much closer to the calculated ones.

2 Preliminary measurements using 500 GHz superconducting integrated receiver

Here we report a construction and first tests of our novel laboratory-purpose sub-mm band tester-receiver. This instrument allows to detect spectrum of radiation in the frequency band of 400-600 GHz from virtually any compact low-power source working at temperatures below 100 K [4]. Both the receiver and a sample are placed in vacuum, inside a laboratory test probe, which is cooled in a standard liquid helium transport dewar. A sensor of the instrument is based on a superconducting integrated receiver (SIR) chip. This SIR chip, besides a quasi-optical SIS mixer, contains an internal electronically tunable superconducting local oscillator, which provides a low-noise operation at the level of about 300 K at central frequency around 500 GHz.

SIS Josephson junctions are known as sensitive detectors in sub-millimeter wavelength range. SIS mixer is presently the most sensitive device for heterodyne reception in the frequency range 100-1000 GHz, its noise temperature is limited only by the fundamental quantum level. The lack of compact, cheap, and easily tunable sum-millimeter local oscillators motivated development of a superconducting oscillator, which can be used as on-chip local oscillator. The best choice of such oscillators is currently flux-flow oscillator based on the unidirectional flow of magnetic fluxons in a long Josephson tunnel junction [3].

The experimental setup consists of a vacuum probe, containing SIR, two IF amplifiers and a bias supply unit [4]. The vacuum space allows to heat a sample installed inside the probe and adjusts the temperature in the range from 4.2 K up to about 100 K without considerable effect on the SIR operating conditions. To protect the magnetic sensitive SIR and sample from external magnetic field, a cryoperm shield of 25 cm long is used. The sample table is thermally isolated from the helium-cold stage and equipped with a heater, thermometer, rf coaxial cable, and w-band waveguide.

To couple the rf power from the emitting sample to the receiver chip with minimal losses, a high precision quasi-optical system of two confocal silicon lens-antennas were developed (Fig. 3. The lenses are identical truncated ellipsoids $R_1 = 5\,\text{mm}$, $R_2 = 5.228\,\text{mm}$ with antireflection coating ($87\,\mu$m thick with $\epsilon \approx 2.9$). Both the lens and its antireflection coating are fabricated with a surface accuracy better than $5\,\mu$m. An infrared filter made of quartz is placed between the lenses to prevent direct IR heating of the receiver chip. The SIR chip and the sample are glued on the flat side of their own lens with soft wax so, that their antennas are within accuracy of $10\,\mu$m in the focus of the corresponding lens.

A low-noise bias supply unit designed in SRON controls the receiver chip. It comprises four independent bias sources: i) for the SIS mixer, ii) for the FFO, iii) and iv) for control lines of the SIS mixer and the FFO. The bias supply unit can be operated manually and/or by a computer. Being under the computer control, the bias supply unit is driven by two data acquisition boards: 16-bit resolution board is used for the FFO and 12-bit resolution board - for the SIS mixer. To avoid the low-frequency ground loops, internal isolated-amplifiers are

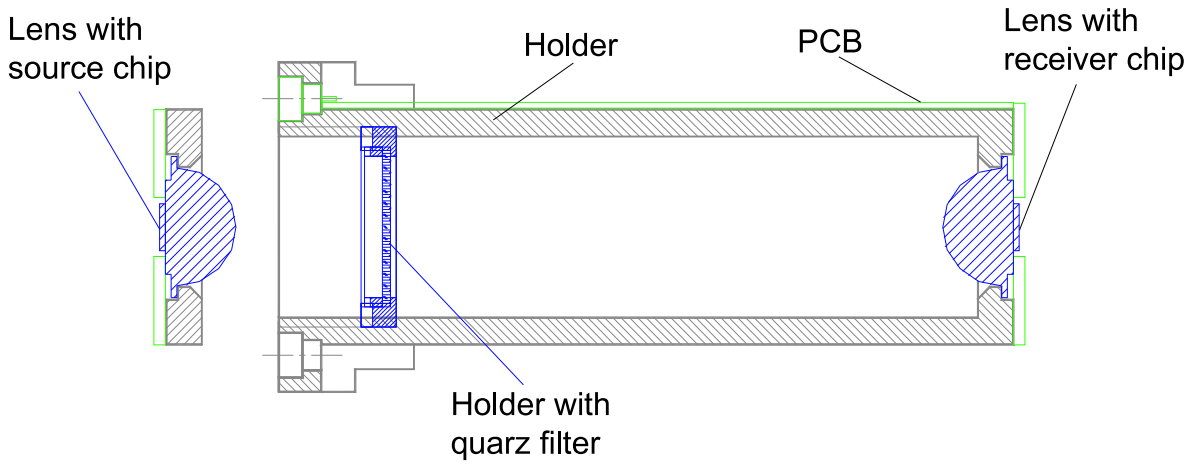

Figure 3: Quasi-optical system of two silicon lens antennas.

used in the bias supply, that also help to reduce the noise caused by the computer.

The superconducting integrated receiver chip is fabricated on a $4 \times 4 \times 0.5\,\mathrm{mm}^3$ silicon substrate using the Nb-AlAlOx-Nb technology with the critical current density about $8\,\mathrm{kAmp/cm}^2$. The receiver chip comprises a SIS mixer ($S = 1 - 1.5\,\mu\mathrm{m}^2$) and a flux-flow oscillator (FFO) as a local oscillator ($450\,\mu$m long and $3\,\mu$m wide). The principle of FFO is the motion of magnetic flux quanta, which density is defined by an external magnetic field. This array of fluxons is driven along the junction by the Lorenz force due to DC bias current. Reaching the end of the long junction, the fluxons provide electromagnetic pulses, which are coupled to a microstrip transmission line. The frequency of the pulses is determined by the Josephson relation $\nu = 2eV/h$. The velocity and density of the fluxons, and thus the power and frequency of the radiation emitted can be adjusted independently by joint effect of bias current and magnetic field. The base electrode of either junctions is used as a control line to produce a local magnetic field. To provide the independent biasing for the SIS mixer and the local oscillator, a DC block is inserted in the transmission line between the FFO and the mixer [5]. For the effective receiving of an external radiation a double-dipole antenna is used with an SIS mixer in the center of it. The combination of the double-dipole antenna and the silicon lens provides the beam of about 10 degrees wide pointed to a sample source. An additional focusing lens can be placed in the optical path at aperture of the receiver head.

The family of the current-voltage characteristics for the FFO in magnetic field and a few examples of pumped IV-curves of the SIS mixer at different FFO frequencies are shown in Fig. 4. We treat the pumping level of the mixer is good when it is in the range of 10-25 % of I_{gap}. It was found theoretically and confirmed experimentally that this pumping level is sufficient for the normal performance of a SIS mixer [6]. The interval of good pumping level and thus the receiver operating range is 20 % of the central frequency of roughly 500 GHz.

In these preliminary experiments our main purpose was detection radiation from long Josephson junction due to Fiske resonances. Because of reflection from the end of the junction it behaves as resonant transmission line. In the presence of the Josephson current at finite voltage there takes place electromagnetic wave radiation with frequency $f = 2eV/h$. This radiation excite resonance modes, which interact with Josephson current. When the Josephson frequency coincides with one of the resonance modes ω there appear step on $I - V$ curve, well known as Fiske steps.

Using the above described SIR setup, we have searched the radiation from a long Josephson

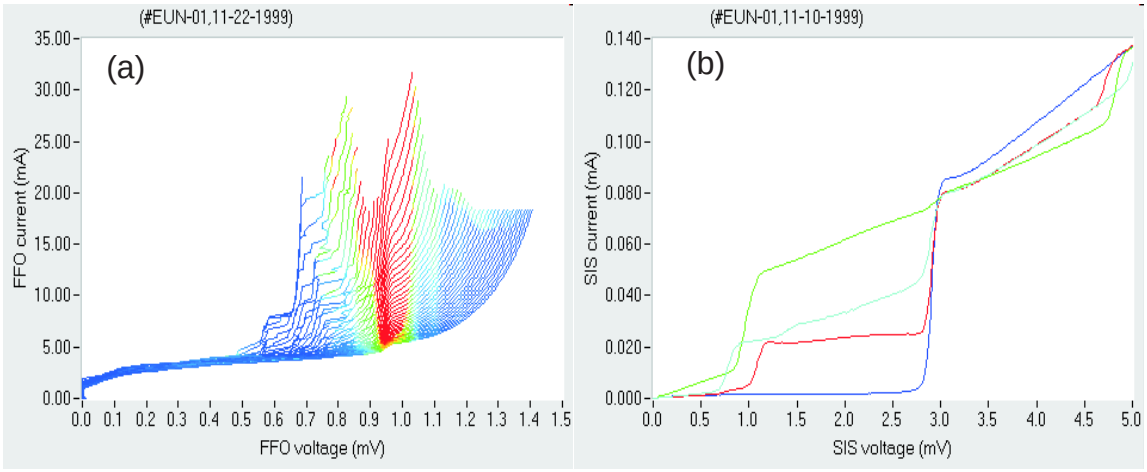

Figure 4: (a) IV curves for the FFO measured at different magnetic fields, (b) the SIS mixer pumped by the FFO at 428, 461, and 500 GHz.

junction. The radiation power from the sample at 4.2 K was found quite small. The response signal was measured only with ac-modulated $I - V$ curve using lock-in Amplifier.

The measured sample consists of two parts: oscillator (long Josephson junction) and dipole antenna coupled to the oscillator, which is used for free-space emission of the radiation from the junction. The layout of the sample is presented in Fig. 5. Coupling between the junction and the antenna in the frequency range of interest was chosen very strong (about $-5\,\mathrm{dB}$), which means that the reflection from the end of the junction coupled to antenna was very small. It turned that this effect considerably reduces the height of the Fiske steps and therefore the power of emitted radiation.

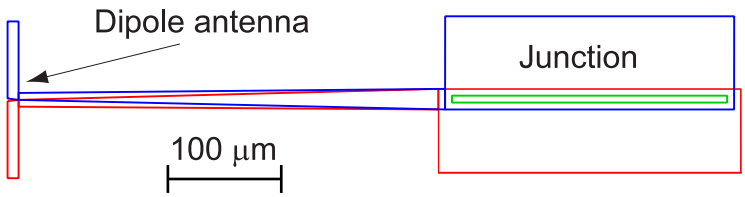

Figure 5: Layout of the long junction coupled to dipole antenna.

For the junctions without antenna the internal radiation power is about $10^{-5}\,\mathrm{W}$, so less than 10 % of this radiation should be enough for detecting it by SIR. Taking this fact into account, we designed now new samples, for which the reflection coefficient from the end of the junction coupled to the antenna is estimated to be in the range $0.8 - 0.9$. As next step to improve the coupling we put the reflector above the sample. The latter reflects radiation in the SIS mixer direction.

3 Conclusions

We reported new layout of samples for experiments using an on-chip radiation detector. Three triangular arrays of small Josephson junctions coupled to detector were designed. In calculation, we hope to succeed to obtain the best matching for the array containing 10 cell

with shunted junctions. For the other arrays the matching coefficients are expected to be relatively good in the frequency range of interest (90-120 GHz). Using the 500 GHz SIR setup, we have also searched the radiation from long Josephson junction coupled via a dipole antenna. The measured radiation power found so far was very small. We designed new samples with revised coupling between antenna and oscillator.

References

[1] P. Caputo, A.V. Ustinov, N.C.H. Lin and S.P. Yukon, Radiation from triangular arrays of Josephson junctions. IEEE Trans. Appl. Supercond., **9**, No.2, pp.4538-4541 (1999)

[2] A.A. Abdumalikov P. Caputo, A. V. Ustinov, Interim Report No.1 on Experiment with mutually coupled arrays of Josephson junctions, contract F61775-00-WE004, September 2001.

[3] J. Qin, K. Enpuku, and K. Yoshida, Flux-flow-type Josephson oscillator for millimeter and submillimeter wave region. IV. Thin-film coupling, J. Appl. Phys. **63**, pp. 1130-1135 (1988).

[4] M. Levitchev, H. Kohlstedt, A.V. Veretennikov, A.M. Shtanyuk, A.V. Ustinov, A.B. Ermakov, G.V. Prokopenko, L.V. Filippenko, S.V. Shitov and V.P. Koshelets, Superconducting Integrated Receiver as 400-600 GHz Tester for Coolable Devices, available on http://www.cplire.ru/html/lab235/pubs/2000-07.pdf

[5] S. V. Shitov, V. P. Koshelets, A. M. Baryshev, I. L. Lapitskaya, L. V. Filippenko, T. de Graauw, H. Shaeffer, H. vad de Stadt, and W. Luinge, A superconducting planar integrated receiver for the frequency range430-480GHz, Proc. 6-th Int. Symp. on Space Terahertz Techn., Pasadena, USA, 324-337, (1995)

[6] V.P. Koshelets and S.V. Shitov, Topical review: Integrated superconducting receivers, Supercond.Sci.Technol. **13** R53-R69. (2000)

Final Report (No. 3)

Experiments with mutually coupled arrays of Josephson junctions*

A.A. Abdumalikov and A. V. Ustinov

Physikalisches Institut III, Universität Erlangen-Nürnberg
D-91054 Erlangen, Germany

* Supported by European Office of Aerospace Research and Development (EOARD)
under Contract F61775-00-WE004

August 2001

Contents

Abstract

Yukon and Lin have proposed a design for an active antenna array based on phase-controlled 2D triangular arrays as oscillators. Synchronization between the oscillators (or subarrays) is provided by a phase shifter consisting of a discrete Josephson junction chain (1D-array). Numerical simulations have shown that, in a certain range of parameters, this circuit can enable radiation beam steering. Earlier we have designed double fin line antenna in order to pick up radiation from the two subarrays. Here we present an outcome of new measurements. Using recently improved 100 GHz setup we have been able to measure radiation from subarrays.

1 Description of the circuit

The realization of an active antenna array involves a rather complex circuit in which several subarrays and phase shifters are coupled through different bias schemes and control lines for local magnetic field for each element of a system. In addition, an appropriate set of antennas has to be included in the circuit in order to pick up radiation. Here we remind details about our earlier design [2] which has been studied again here.

The subarray: As a subarray we have taken double row square cell triangular array. Each row consists of 13 cells. Superconducting probes are placed across each row so that the individual row voltages can be measured. The elementary cell contains four small Josephson junctions. The horizontal branch consists of 2 junctions connected in series. The junction size is about 9 μm^2. The cell size is about 160 μm^2. The bias current flows through bias resistors and tabs. Tabs can be two types with and without horizontal junctions. In order to keep symmetry we have designed tabs without horizontal junctions. The sketch of the subarray is presented in Fig. 1.

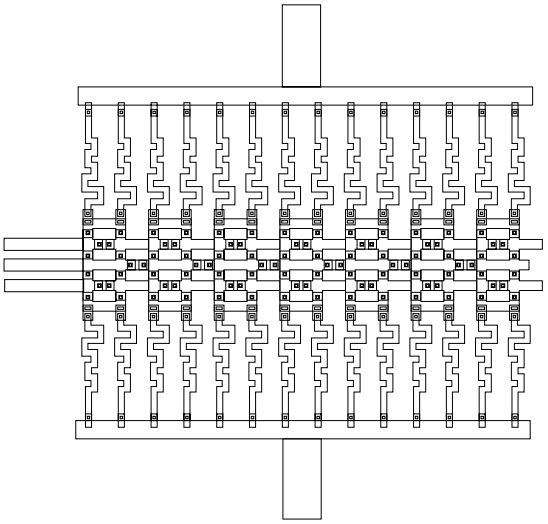

Figure 1: Layout of the subarray consisting of two rows of 13 cells.

The phase shifter: For synchronize the oscillations in two different subarrays they should be mutually coupled either directly or via some phase shifter. The first case corresponds for the case of a twice long array. The phase shifters not only synchronize but makes some phase shift between the oscillations in the coupled subarrays. In this case we will have enhanced radiation, at the output.

As a phase shifter we have used a ladder of Josephson junctions with 16 cells. The phase shifter was designed to have same cell size (160 μm^2) and junctions (9 μm^2) as the subarrays. Elementary cell contains four junctions. A sketch of the phase shifter with 16 cell is shown in Fig 2.

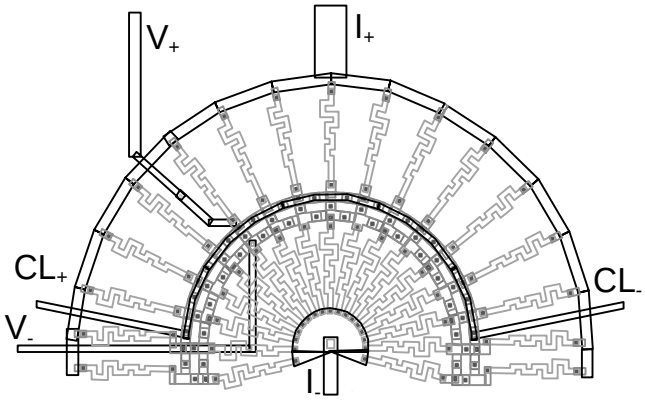

Figure 2: Layout of the semi-circular phase shifters consisting of 16 cells.

Double fin line antenna: In order to pick up radiation from the two subarrays we used double fin line antenna. Its both parts are in parallel and take radiation from different subarrays. The outer electrodes of the antenna excites electromagnetic wave in a wave guide.

2 Measurements

The active array we have measured contains two subarrays, phase shifter and double fin line antenna. In order to simplify biasing scheme the phase shifter and two subarrays were designed without galvanic coupling. In the circuit the phase shifter is aligned not directly to one of the rows of the subarray, but to the inner biasing tabs. In this case one would expect less influence of the phase shifter on the subarrays. The two subarrays have common lead for biasing, which is also simplifies the whole biasing scheme and, at the same time, allows us to supply the arrays with same current. With such a biasing the fluxon chain exciting one of the subarrays goes through the phase shifter and enters into the other subarray. The fin line antenna is used for coupling the emitted radiation to a waveguide. The layout of the measured circuit is presented in Fig. 3.

First we started with dc characterization of the subarrays. Fig. 4(a) shows the current voltage characteristics of one of the subarrays. In Fig. 4(b) we have presented the pattern of the critical current vs. external perpendicular magnetic field. In both pictures the red lines correspond to one row, while the black ones to another row. We can see that the dc characteristics of the rows are similar.

We have performed radiation measurement using room temperature superhetherodyne receiver. Recently we modified our setup to be able to generate rf power in the frequency range of the detection (78-118 GHz). By applying this radiation to our circuit we have observed Shapiro and photon assisted tunneling steps induced on the subarrays I-V curve. By changing the frequency of the external radiation we can precisely determine the frequency range where to search for a radiation from our sample. By doing this we have determined that the radiation frequency lies in the range 85-90 GHz. Further we changed the local oscillator frequency in this range. Measured power with corresponding I-V curve of one row is shown in Fig. 5. From this curve we have determined that the radiation frequency is about 86.5 GHz. We could not measure spectrum of the radiation because of its low power.

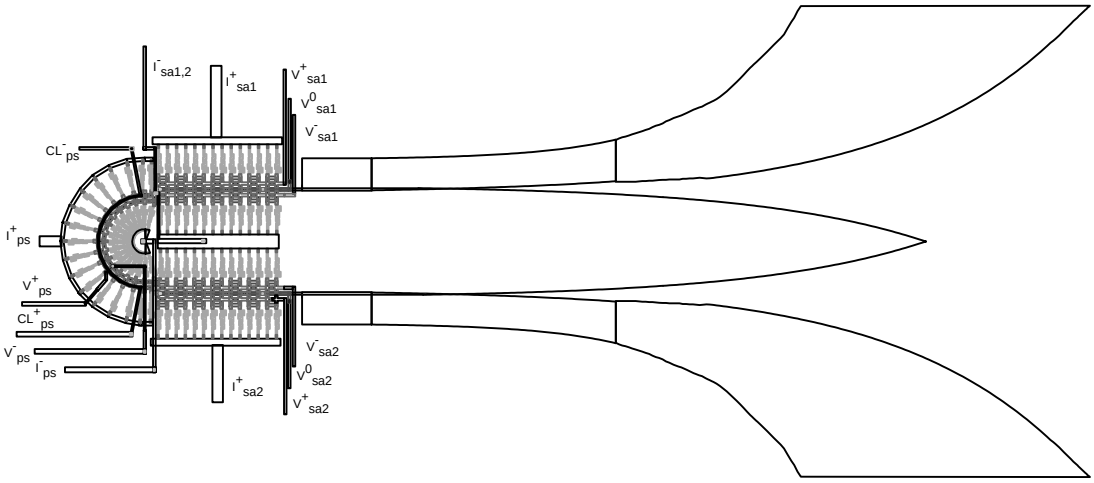

Figure 3: Layout of active antenna with galvanically decoupled phase shifter.

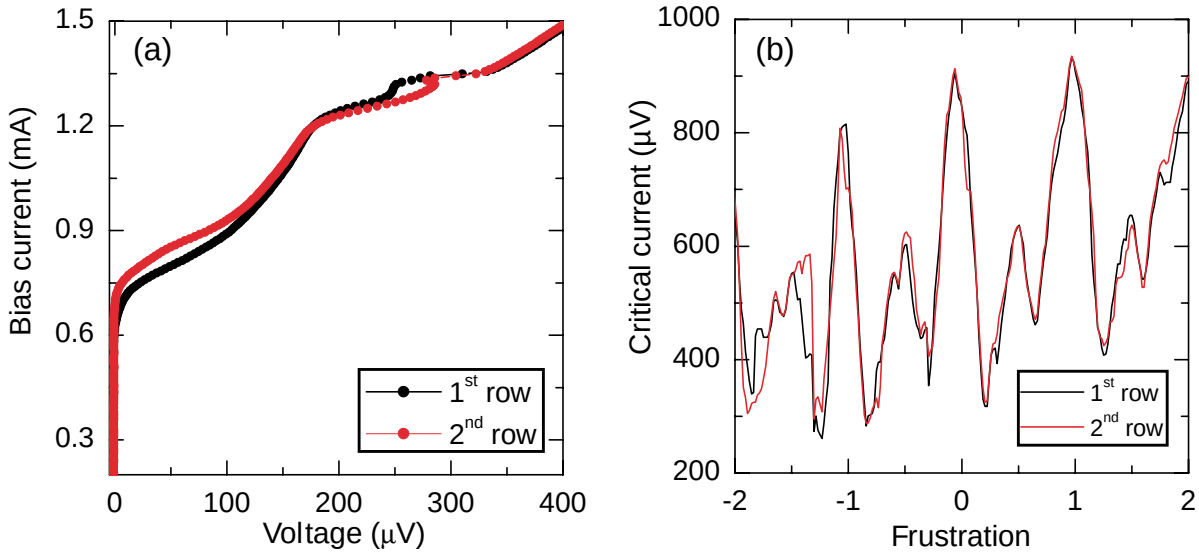

Figure 4: DC characteristics of the first subarray: I-V curve at half frustration (a), critical current vs. frustration.

Measured data analysis show that the radiation power does not depend on the current through phase shifter (Fig. 6(a)). At least the power change due to phase shifter current is less than noise. We could not detect any change even with large time averaging. The radiation power versus external magnetic field is shown in Fig. 6(b). The power dependence on a magnetic field is smeared by noise, however with large averaging we have noticed a little effect.

3 Conclusions

We have tested circuits based on 2 row arrays of Josephson junctions mutually coupled by a phase shifter. We have finally succeeded to measure radiation from the two subarrays. The detected radiation frequency is about 86.5 GHz. It was observed that the radiation power does not depend on phase shifter, or at least its dependence is very weak. Several points still remain to be clarified. Under question is the operation of phase shifter and subarray

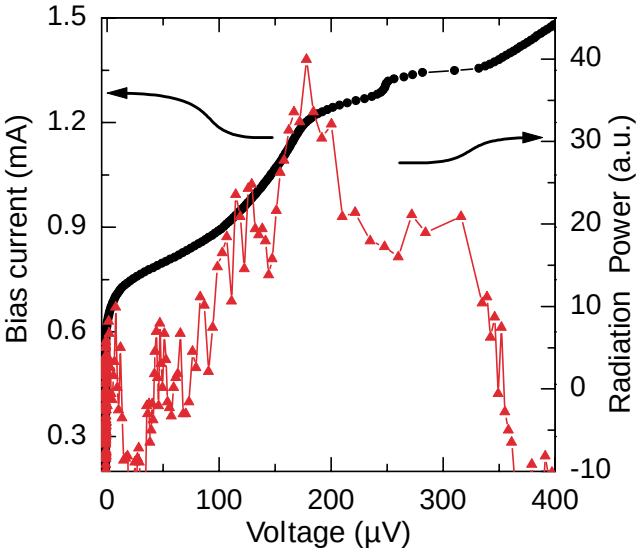

Figure 5: I-V curve (black) and detected power (red) in external magnetic field corresponding to the half flux quantum.

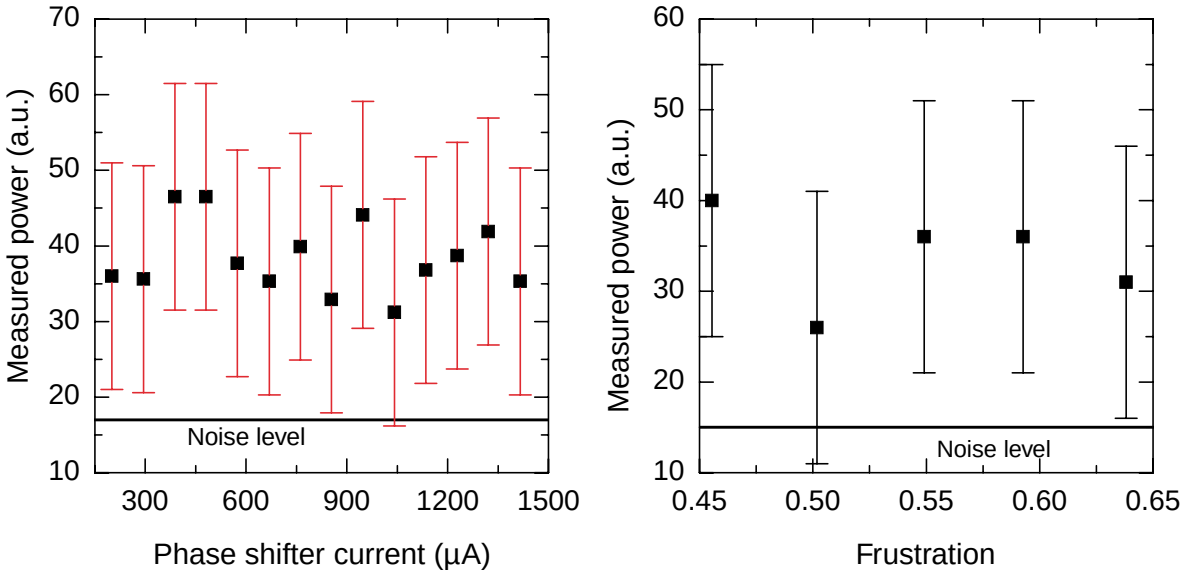

Figure 6: Detected power dependence on phase shifter current (a) and on external perpendicular magnetic field (b).

alignment.

References

[1] N.C.H. Lin and S.P. Yukon, Josephson Junction Phased Arrays, IEEE Trans. Appl. Supercond., **9**, No.2, pp.4533-4537 (1999)

[2] P.Caputo and A. V. Ustinov, Final Report on Experiments with Mutually Coupled Arrays of Josephson Junctions, contract F61775-99-WE012, March 2000